EFFECTS OF CARDIAC GATING ON fMRI OF THE HUMAN AUDITORY SYSTEM

by

ANDREW R. DYKSTRA

B.S., Electrical Engineering – Audio Option (2005)
University of Miami, Coral Gables, FL

SUBMITTED TO THE DEPARTMENT OF ELECTRICAL ENGINEERING AND COMPUTER SCIENCE IN PARTIAL FULFILLMENT OF THE REQUIREMENTS FOR THE DEGREE OF

MASTER OF SCIENCE IN ELECTRICAL ENGINEERING AND COMPUTER SCIENCE

at the

MASSACHUSETTS INSTITUTE OF TECHNOLOGY

September 2008

Author _____
Department of Electrical Engineering and Computer Science
August 29, 2008

Certified by _____
Jennifer R. Melcher
Assistant Professor of Otology & Laryngology and HST, Harvard Medical School
Thesis Supervisor

Certified by _____
Louis D. Braida
Henry Ellis Warren Professor of Electrical Engineering
Faculty Member, HST-SHBT
Thesis Supervisor

Accepted by _____
Professor Terry P. Orlando
Chair, Department Committee on Graduate Students

EFFECTS OF CARDIAC GATING ON fMRI OF THE HUMAN AUDITORY SYSTEM

by

Andrew R. Dykstra

Submitted to the Department of Electrical Engineering and Computer Science on August 29, 2008

in partial fulfillment of the requirements for the degree of

Master of Science in Electrical Engineering and Computer Science

Abstract

Guimaraes et al. (1998) showed that sound-evoked fMRI activation in the auditory midbrain was significantly improved by a method which reduces image signal variability associated with cardiac-related brainstem motion. The method, cardiac gating, synchronizes image acquisition to a constant phase of the cardiac cycle. Since that study, several improvements to auditory fMRI have been made, and it is unclear whether cardiac gating still yields worthwhile benefits. The present study re-evaluated the effects of cardiac gating for detecting fMRI activation with current auditory fMRI standards. In 11 experiments, we directly compared fMRI activation for images acquired with a fixed repetition time (ungated) vs. those acquired by triggering image acquisition (gated) to the oxygen saturation at the fingertip (SpO2), an indirect measure of cardiac activity. Three of these experiments compared the effects of gating with the SpO2 signal vs. gating with the R-wave of the electrocardiogram (ECG). fMRI activation was routinely detected at all levels of the auditory pathway from the cochlear nucleus to the auditory cortex. Compared to ungated acquisitions, cardiac gating with the SpO2 reduced image signal variability in all centers of the auditory system and increased the magnitude of activation in the inferior colliculus ($p < 0.01$) and medial geniculate body ($p < 0.1$). Simultaneous measurements of the SpO2 and ECG indicated that the peak of the SpO2 signal followed the ECG R-wave by approximately 400 ms, placing early images in a motion-stable phase of the cardiac cycle during SpO2-gated experiments. This may account for the fact that image signal variability with SpO2-gated acquisitions was always lower than with ECG-gated acquisitions. That sound-evoked activation could be regularly detected without cardiac gating indicates that gating may not be worth the minimal experimental complexity it entails. However, in experiments attempting to measure responses to sounds that evoke small changes in fMRI signal, especially in the auditory midbrain or thalamus, or when one interested in individual variability rather than group averages, gating may prove extremely beneficial.

Thesis Supervisor: Jennifer R. Melcher
Associate Professor of Otolaryngology, Harvard Medical School

Thesis Supervisor: Louis D. Braida
Henry Ellis Warren Professor of Electrical Engineering, MIT

Contents

1 Introduction

In the early years of functional neuroimaging, fMRI studies focused mainly on task-related activity of the cerebral cortex, in large part because detection of sub-cortical activation, especially in the brainstem, was unreliable. The difficulty in imaging sub-cortical nuclei arises from a combination of their small size (on the order of a single voxel at the typical in-plane resolution of fMRI – $3mm^2$), motion of the brainstem due to its proximity to large blood vessels, and flow of surrounding cerebrospinal fluid (Poncelet et al., 1992). In addition, imaging auditory nuclei in general was problematic because of the saturating effect of acoustic scanner noise on neural activity in the auditory system and the resulting suppression of fMRI activation from sound stimuli (Hall et al., 2000; Elliot et al., 1999; Bandettini et al., 1998; Ulmer et al., 1998a; 1998b; Ravicz et al., 2000; 2001). The effects of scanner noise have been mitigated using "sparse" or clustered imaging paradigms (Edmister et al., 1999; Hall et al., 1999) in which image volumes are acquired in a brief cluster with a long silent period between clusters. The effects of brainstem motion on detecting activation in brainstem centers have been mitigated by synchronizing image acquisitions to a particular phase of the subject's cardiac cycle ("cardiac gating") instead of acquiring images at fixed intervals (Guimaraes et al., 1998). The original study which proposed this technique was performed at 1.5-Tesla field strength and demonstrated that cardiac gating could determine whether or not one is able to detect activation in the auditory midbrain (i.e., the inferior colliculus). Since its introduction, this method has been used in many studies of the small auditory nuclei of the brainstem (e.g. Harms and Melcher, 2002; Melcher et al., 2000; Devlin et al., 2006; Griffiths et al., 2001; Backes and van Dijk, 2002) as well as brainstem nuclei in other sensory pathways (Zhang et al., 2006; Mainero et al., 2007; Dubois and

Cohen, 2000). However, recent studies performed at higher field strengths have readily measured brainstem activation without using cardiac gating or any other method to reduce image signal variability caused by brainstem motion (Budd et al., 2003; Kovacs et al., 2006; personal observations of the authors). These observations raise the following questions: Does cardiac gating significantly improve the detection of subcortical activation when used with current fMRI methods? If so, under what circumstances is the benefit sufficient to warrant the additional experimental and post-processing complexity that cardiac gating entails?

The present study reexamined the effect of cardiac gating on activation detection in a study design similar to that of Guimaraes et al. (1998). We directly compared activation measured using cardiac gating with activation measured using a fixed interval (TR) between image clusters (not the case with gating because heart rate varies over time). However, our study also differed from Guimaraes et al. (1998) in several important ways. First, images were acquired at 3-Tesla instead of 1.5 Tesla. Second, we imaged several auditory nuclei from cochlear nucleus through auditory cortex while mitigating scanner noise using clustered volume acquisitions. Third, in the gated condition, we synchronized image acquisitions to the oxygen concentration (SpO2) in the fingertip as a simpler alternative to the electrocardiogram (ECG). We recognized that triggering from the more-sluggish SpO2 signal might lead to less consistent triggering with respect to cardiac phase, and thus compromise any benefits from gating. We assessed whether this was the case by collecting ECG- as well as SpO2-gated data in some experiments. Finally, as it has never been quantitatively examined, we measured the delay between the peak of the ECG and SpO2 waveforms. .

The results of the present study demonstrate that cardiac gating via the SpO2 signal improves detection of sound-evoked activation in auditory midbrain and thalamus. We use the data to suggest guidelines for deciding if gating is worthwhile in a given experimental context.

2 Methods

Ten subjects participated in these experiments. Nine were imaged once, and one twice, for a total of 11 imaging sessions. All subjects had normal hearing (25 dB HL or less at all standard audiometric frequencies from 250 Hz to 8 kHz) and no tinnitus. No subject reported a history of neurological illness. Approval for the experiments was granted by the Institutional Review Boards at the Massachusetts Eye and Ear Infirmary, Massachusetts Institute of Technology, and the Massachusetts General Hospital. Written informed consent was obtained prior to participation.

2.1 Acoustic Stimulation

Broadband noise (0-10 kHz) was presented binaurally at 50dB SL (referenced to the monaural threshold for each ear) via insert piezo-electric headphones with noise-reducing foam earplugs. Detection threshold was measured in the scanner room while no images were being acquired. The patient cooling fan was off during threshold measurement and during functional imaging. The scanner coolant pump was left on for technical reasons in all but two subjects. Stimuli were presented in a block paradigm with constant length "sound on" epochs (32 sec) but variable length "sound off" epochs (30 - 38 sec) such that the timing of image acquisition relative to the stimulus was staggered by ~2 seconds across "on" epochs. The staggered sampling enabled synthesis of image signal time courses with 2-second resolution despite the original,

long (i.e., ~8 second) inter-image interval (Belin et al. 1999; Harms et al. 2005). In each imaging session, the same amount of imaging time was devoted to each study condition: ungated, SpO2-gated and, for the three experiments employing it, ECG-gated. Participants were asked to keep as still as possible and to listen

2.2 Imaging

Image data were collected using a 3-Tesla Siemens TIM Trio and 12-channel head coil (Matrix). Participants were placed head-first supine into the scanner and immobilized using padding placed on either side of the head.

Contiguous sagittal images of the whole head were acquired and used to select a volume comprising 10 slices for functional imaging. In 8 out of 11 imaging sessions, the slices were oriented parallel to a plane intersecting the inferior colliculi and cochlear nuclei (identified as described in Hawley et al., 2005). In the 3 remaining experiments, the slices were parallel to a plane intersecting the inferior colliculi and posterior Heschl's gyri. In all but one case, the orienting slice (containing IC and CN or IC and HG) was the second from most posterior (most posterior in remaining case). In all cases, the auditory pathway from CN through MGB was contained in slices 2 - 4 (numbered from posterior to anterior beginning with "1").

Figure 1 shows the functional imaging paradigm. Functional imaging used blood-oxygenation level-dependent (BOLD) contrast (in-plane resolution = 3.1 x 3.1 mm^2; slice thickness = 6 mm; distance factor = 33%; FoV = 200 x 200 mm^2; flip angle = 90°; echo time = 30ms). Images of the 10-slice volume were acquired in a brief cluster (600 ms) every 8 (ungated) or approximately 8 (gated) seconds. were acquired with a repetition time (TR) of 8 seconds for ungated-TR runs and approximately 8 seconds (7.5 seconds + 1 heartbeat) for gated-

TR runs with clustered volume acquisitions (Edmister et al. 1999, Hall et al. 1999) with a cluster length of 600ms. Thirty-five image clusters were acquired for all 10 slices of interest during one ungated-TR run, while approximately 35 (due to the variability in TR) image clusters were acquired in one gated-TR run.

For gated-TR runs, image acquisition began immediately after a peak in either the pulse oximeter or ECG R-wave was detected. In three experiments comparing ECG and SpO2 gating, the ECG and SpO2 signals were measured during the ungated runs using an INVIVO Magnitude 3150M (Intermagnetics General Corporation, Latham, NY) in order to quantify the delay between the two signals and examine how that delay might effect the derived detection benefit from cardiac gating.

2.3 Detecting Activation

Images were corrected for subject motion using the Statistical Parametric Mapping software package (SPM2; Friston et al., 1995), co-registered to the first functional images of the session, and corrected for linear and quadratic drift in signal intensity within a run on a voxel-wise basis. T1 correction was applied to each gated run (Guimaraes et al., 1998) although, as expected, it had little effect on image signal because of the long TR used in the current study. Images were normalized such that the time-averaged signal intensity had the same value across runs in order to eliminate artificial intensity discontinuities. All data for a single condition (ungated, SpO2-gated, ECG-gated) were concatenated, forming a single data set used for all further analyses. Activation was detected using a student's t-test (on a voxel-wise basis) between images while the stimulus was on and those acquired while the stimulus was off. A

voxel was considered activated if the resulting p-value was below 0.01 (uncorrected for multiple comparisons).

2.4 Region of Interest Analysis

The following regions-of-interest (ROIs) were defined as in Hawley et al. (2005) and Harms and Melcher (2002): cochlear nucleus, superior olivary complex, inferior colliculus, medial geniculate body. Three ROIs were also defined on the superior temporal plane: Heschl's gyrus (HG), planum temporale (PT) and planum polare (PP). The HG ROI comprised the first Heschl's when there were two. Areas medial to Heschl's gyrus were assigned to PP and those lateral to HG, including a second Heshl's gyrus if there was one, was assigned to the PT ROI. Similar patterns of results for sub-cortical structures were obtained for two separate ROI analyses.

2.5 Quantifying Activation

The following were quantified for each condition (ungated, SpO2 gated, ECG gated) based on the logical OR of active voxels ($p < 0.01$) within each ROI: (1) the average T-statistic, (2) the average percent signal change in voxel intensity between the "on" and "off" conditions, (3) the average standard deviation in signal intensity during the "on" condition, and (4) the average standard deviation in signal intensity during the "off" condition. These quantities were also assessed for the active voxels in the different conditions individually. To assess the effects of cardiac gating upon these four measures, we used non-parametric sign and signed-rank tests and defined statistical significance as $p < (\alpha = 0.05)$.

3 Results

In both the ungated and SpO2 gated conditions, activation from the sound stimulus was routinely detected in the following auditory centers: cochlear nucleus, superior olivary complex, medial geniculate body, Heschl's gyrus, planum temporale, and planum polare. Figure 2 shows activation maps for both ungated and gated conditions chosen because any change in T-statistic between the ungated and gated conditions was near the mean across subjects.

Figures 3 and 4 and Table 1 summarize the difference between the ungated and SpO2 gated conditions for every subject and brain structure. The analyzed voxels in each ROI were the same for the ungated and gated conditions and comprised the OR of active voxels during the two conditions. All structures showed a significant reduction in image noise during both sound on and off periods, as assessed by signal standard deviation [$p < 0.05$ for signed-rank test (one asterisk) or both signed-rank and sign tests (two asterisks)]. The reduction is apparent by eye in the time courses of Figures 5 and 6, particularly for the inferior colliculus. In the inferior colliculus, gating produced a significant increase in T score, a measure of signal detectability. The T score in MGB showed an increasing trend ($p < 0.1$), while the remainder of the structures showed no difference in T scores between the gated and ungated conditions. There was no difference in percent signal change between ungated and gated conditions in any structure. An alternative analysis in which the relevant measures for each condition were calculated based on the active voxels for that condition yielded an essentially identical pattern of results: a reduction in standard deviation with gating for all structures, a significant increase in T score for the inferior colliculus with gating, and a trend toward increased T score in MGB.

In three experiments, the efficacy of gating with the SpO2 signal was directly compared with that of gating with the ECG. T-scores were always highest (and signal variability lowest) when using the SpO2, followed by the ECG and ungated conditions, respectively. This may be due to the fact that gating with the SpO2 or EG signals places the first images in different phases of the cardiac cycle. As seen in Figure 7, the peak of the SpO2 signal is delayed by about 400 ms relative to the R wave of the ECG.

4 Discussion

When used in conjunction with current auditory neuroimaging methods, cardiac gating significantly increased T-scores in the inferior colliculus and tended to increase it in MGB and HG??. In the structures which received a benefit from cardiac gating, the benefit resulted from reduced signal variability in both the "on" and "off" conditions with no corresponding change in percent signal change. T score, and thus the detectability of activation was never reduced by gating.

Because previous studies comparing ungated and gated image acquisition used the ECG signal, we wondered whether using the SpO2 signal would adversely affect our results. However, gating with the SpO2 signal yielded higher T-scores and lower signal variability than gating with the ECG. This is likely due to the fact that the SpO2 signal is delayed by about 400 ms relative the ECG, putting the first images acquired in a relatively stable phase of the cardiac cycle (Poncelet et al., 1992). The downside of gating with the SpO2 is that image acquisition later in the volume might have fell beyond the next cardiac cycle, and thus were not truly gated.

Some of these images included the anterior portions of auditory cortex, and this may have biased our results in these structures towards not showing any benefit from gating.

The fact that we observed a detection benefit from gating in some structures but not others may be due to such factors as direction of brainstem and cortical movement (e.g. through-plane vs. in-plane) or flow of oxygenated or deoxygenated blood in vessels (e.g. posterior cerebral artery, middle cerebral artery) adjacent to auditory nuclei.

4.1 When to use Cardiac Gating

Although cardiac gating requires some minimal experimental complexity when compared with traditional ungated acquisitions, the technique may prove especially beneficial under certain experimental conditions (e.g. if one wishes to examine the neural response to events that produce small changes in BOLD signal or is interested in individual subject or patient variability). To gain some quantitative intuition for this, we artificially reduced the percent signal change between the noise-on and noise-off conditions for both the ungated and gated paradigms in each subject (IC) and determined at what percent signal change we could no longer detect activation at the 0.01 level. As seen in Figure 8, the percent signal change at which activation could still be detected was always lower when cardiac gating was used (mean minimum percent signal, ungated = 0.40 ± 0.11; gated = 0.29 ± 0.09). These signal changes are comparable to those evoked by low-sound-level, low-bandwidth, or low-rate stimuli (Sigalovsky and Melcher, 2006; Hawley et al., 2005; Harms and Melcher, 2002). Gating may therefore provide more reliable measures of neural activation in psychophysical detection or discrimination experiments as well as when one is interested in describing individual or patient variability to sounds that elicit just-detectable activation.

4.2 Comparison with Previous Imaging Studies of Cardiac Gating

Guimaraes et al. (1998), using a 1.5 Tesla scanner and acquiring data from a single slice intersecting both the inferior colliculi and Heschl's gyri with a short TR of either 2s (ungated) or ~2s (gated) using the ECG for triggering with a 400ms delay between trigger and acquisition, showed that under those experimental conditions, cardiac gating was a determining factor of whether activation was detected in the inferior colliculi of some subjects. Cardiac gating also increased the significance of fMRI activation in the auditory cortex. However, while increased activation in the brainstem was a result of a reduction in signal variability, increased activation in the auditory cortex was a result of larger percent signal changes. We replicated the first result under different imaging conditions [3-Tesla scanner, long TR (ungated TR = 8s; gated TR ≈ 8s)], pulse-ox triggering with no delay between the trigger and the start of image acquisition, multi-slice clustered-volume acquisitions] while also expanding on it by showing increased activation in both the inferior colliculi and the medial geniculate bodies resulting from reductions in signal variability. While we did observe some reductions in signal variability in the cochlear nuclei and superior olivary complexes, gating did not increase activation in these structures due to a corresponding tendency of gating to reduce the percent signal change. That we observed the largest variability reductions in brainstem structures (IC and MGB) and less reduction in the cochlear nuclei, superior olivary complexes, and auditory cortices strengthens Guimaraes et al.'s and others' (Zhang et al., 2006; Malinen et al., 2006) conclusion that gating improves activation detection in the brainstem by mitigating the noise associated with pulsatile motion caused by semi-periodic blood flow and also indicates that cardiac gating, when performed correctly, still

provides a substantial benefit in detecting activation in subcortical auditory structures with present auditory fMRI methods.

Malinen et al. (2006), using a pulse-oximeter with a 300ms delay between trigger and start of acquisition, showed more reliable activation detection in secondary somatosensory cortex by using cardiac gating. This improvement was the result of reduced signal variability in the regions of interest with no corresponding differences in percent signal change. Malinen et al.'s (2006) slice selection did not cover primary sensory cortex. It is unclear why they observed detection benefits in cortical regions and we did not even though signal variability in these regions was reduced in both their study and ours.

4.3 Mechanisms behind Reduced Variability in Cortical ROIs

Contrary to the brainstem, it is still unclear why gating might result in reduced signal variability in cortical regions. It could be that motion of the cortex (Poncelet et al., 1992), even in regions with largely homogenous hemodynamic responses to stimulation, results in increased signal variability throughout the brain. The largest variability would be expected in regions containing larger arteries. That we observed the largest variability reductions in the brainstem, adjacent to the posterior cerebral arteries and a smaller but still significant reduction in Heschl's gyrus, adjacent to the middle cerebral artery, supports this idea. Another possibility is that blood flow, even in the absence of associated pulsatile motion, is a source of signal variability on the short time scales between different phases of cardiac activity (Krüger and Glover, 2001). If this were true, we would again expect to see variability reductions throughout the brain by cardiac gating. Our findings tend to support both ideas, and we cannot dissociate between them with our data. In addition, it has been shown that *physiological* noise, including fluctuations in cerebral

metabolism, blood flow, blood volume, and quasiperiodic cardiac and respiratory fluctuations (1) dominate image noise at 3 Tesla (Krüger and Glover, 2001), suggesting that the best avenue for reducing signal variability is by methods targeting physiological noise, like cardiac gating and/or retrospective correction (Le and Hu, 1996; Glover et al., 2000) for both the cardiac and respiratory cycles.

4.4 Cardiac Gating vs. other Noise-reduction Methods

Zhang et al. (2006) directly compared fMRI activation between runs with and without using cardiac gating in the detection of activation in the trigeminal nuclei of the brainstem. Zhang et al. (2006) used the peak of the R-wave in the ECG to trigger scans in several different acquisition paradigms including ungated with a TR of 3s, gated with a TR of 3 heartbeats with and without T1 correction, gated with a TR of 9 heartbeats and no T1 correction, and a dual-echo acquisition for T2* mapping to eliminate the effects of TR variability on signal recovery. They found cardiac gating to be beneficial in that it improved the detection hit rate in all structures of interest by reducing signal variability. The largest hit rate, however, was obtained using a variant of a multi-echo, single-shot sequence (Wiggins and Norris, 1998; Speck and Hennig, 1998; Posse et al., 1999; Schulte et al. 2001) which maps T2* on a voxel-wise basis. Such a sequence is advantageous because it eliminates (1) variability associated with signal drift over long imaging sessions, (2) inter-subject and regional T2* differences, and (3) the need to correct for T1-related variability associated with a variable TR. Indeed, Posse et al. (1999) reported improved functional contrast in the visual cortex using this sequence. The disadvantage of this technique lies in the time it takes to acquire images at multiple echo-times. If one wants to be sure that all slices of interest are truly cardiac gated, placed in a motion- and blood-flow-stable

phase of the cardiac cycle, less slices can be obtained with multi-echo sequences than with conventional BOLD fMRI. In addition, for auditory fMRI, longer image acquisitions, and more echoes, produce more acoustic noise which might contaminate the measurement of the stimulus-related hemodynamic response. Nonetheless, it would be interesting to use a multi-echo sequence with current auditory fMRI methods to compare its efficacy in detecting auditory activation in the brainstem and elsewhere.

5 Conclusion

With current auditory fMRI methods including clustered volume acquisitions, long repetition time, and high field strength, recent studies have obtained reliable subcortical activation in auditory structures without using cardiac gating while others (e.g. Thompson et al., 2006; Sigalovsky and Melcher., 2006; Griffiths et al., 2001; Rinne et al., 2007) have assumed that cardiac gating is a beneficial methodological modification without which detection of activation in subcortical auditory nuclei might not be possible. Many have also assumed that if a study is not concerned with subcortical structures, then gating is not necessary (e.g. Gutschalk et al., 2007; Wilson et al., 2007; Hall et al., 2005). It does seem that cardiac gating provides a benefit in detecting hemo-dynamic activation in the auditory brainstem and thalamus, and possibly the cortex.. Gating would be particularly useful for situations in which the contrast-to-noise ratio is inherently low and/or when one is interested in the variability of auditory activation across individual subjects, particularly for such clinical conditions as schizophrenia or tinnitus.

6 Acknowledgements

We thank Dr. Euicheol Nam, Wendy Gu, Dr. Randy Gollub, and Dr. Elif Ozdemir for helpful comments and assistance with data collection. We thank Barbara Kiang for assistance in figure preparation. Supported by NIH T32-DC00038 and the Harvard-MIT Division of Health Sciences and Technology.

7 References

Backes, W. H. and P. van Dijk (2002). "Simultaneous sampling of event-related BOLD responses in auditory cortex and brainstem." Magn Reson Med **47**(1): 90-6.

Belin, P., R. J. Zatorre, et al. (1999). "Event-related fMRI of the auditory cortex." Neuroimage **10**(4): 417-29.

Devlin, J. T., E. L. Sillery, et al. (2006). "Reliable identification of the auditory thalamus using multi-modal structural analyses." Neuroimage **30**(4): 1112-20.

DuBois, R. M. and M. S. Cohen (2000). "Spatiotopic organization in human superior colliculus observed with fMRI." Neuroimage **12**(1): 63-70.

Edmister, W. B., T. M. Talavage, et al. (1999). "Improved auditory cortex imaging using clustered volume acquisitions." Hum Brain Mapp **7**(2): 89-97.

Friston, K. J., A. P. Holmes, et al. (1995). "Statistical parametric maps in functional imaging: A general linear approach." Hum Brain Mapp **2**(4): 189-210.

Glover, G. H., T. Q. Li, et al. (2000). "Image-based method for retrospective correction of physiological motion effects in fMRI: RETROICOR." Magn Reson Med **44**(1): 162-7.

Griffiths, T. D., S. Uppenkamp, et al. (2001). "Encoding of the temporal regularity of sound in the human brainstem." Nat Neurosci **4**(6): 633-7.

Guimaraes, A. R., J. R. Melcher, et al. (1998). "Imaging subcortical auditory activity in humans." Hum Brain Mapp **6**(1): 33-41.

Hall, D. A., D. J. Barrett, et al. (2005). "Cortical representations of temporal structure in sound." J Neurophysiol **94**(5): 3181-91.

Hall, D. A., M. P. Haggard, et al. (1999). ""Sparse" temporal sampling in auditory fMRI." Hum Brain Mapp **7**(3): 213-23.

Harms, M. P., J. J. Guinan, Jr., et al. (2005). "Short-term sound temporal envelope characteristics determine multisecond time patterns of activity in human auditory cortex as shown by fMRI." J Neurophysiol **93**(1): 210-22.

Harms, M. P. and J. R. Melcher (2002). "Sound repetition rate in the human auditory pathway: representations in the waveshape and amplitude of fMRI activation." J Neurophysiol **88**(3): 1433-50.

Hawley, M. L., J. R. Melcher, et al. (2005). "Effects of sound bandwidth on fMRI activation in human auditory brainstem nuclei." Hear Res **204**(1-2): 101-10.

Kiang, N. Y., B. C. Fullerton, et al. (1984). Artificial stimulation of the auditory system. Advances in Audiology, vol. 1. M. Hoke. Basel, Switzerland, Karger: 6-17.

Kovacs, S., R. Peeters, et al. (2006). "Activation of Cortical and Subcortical Auditory Structures at 3 T by Means of a Functional Magnetic Resonance Imaging Paradigm Suitable for Clinical Use." Investigative Radiology **41**(2): 87-96.

Kruger, G. and G. H. Glover (2001). "Physiological noise in oxygenation-sensitive magnetic resonance imaging." Magn Reson Med **46**(4): 631-7.

Le, T. H. and X. Hu (1996). "Retrospective estimation and correction of physiological artifacts in fMRI by direct extraction of physiological activity from MR data." Magn Reson Med **35**(3): 290-8.

Levine, R. A., J. C. Gardner, et al. (1993). "Binaural auditory processing in multiple sclerosis subjects." Hear Res **68**(1): 59-72.

Mainero, C., W. T. Zhang, et al. (2007). "Mapping the spinal and supraspinal pathways of dynamic mechanical allodynia in the human trigeminal system using cardiac-gated fMRI." Neuroimage **35**(3): 1201-10.

Malinen, S., M. Schurmann, et al. (2006). "Improved differentiation of tactile activations in human secondary somatosensory cortex and thalamus using cardiac-triggered fMRI." Exp Brain Res **174**(2): 297-303.

Melcher, J. R., I. S. Sigalovsky, et al. (2000). "Lateralized tinnitus studied with functional magnetic resonance imaging: abnormal inferior colliculus activation." J Neurophysiol **83**(2): 1058-72.

Micheyl, C., R. P. Carlyon, et al. (2007). "The role of auditory cortex in the formation of auditory streams." Hear Res **229**(1-2): 116-31.

Poncelet, B. P., V. J. Wedeen, et al. (1992). "Brain parenchyma motion: measurement with cine echo-planar MR imaging." Radiology **185**(3): 645-51.

Posse, S., S. Wiese, et al. (1999). "Enhancement of BOLD-contrast sensitivity by single-shot multi-echo functional MR imaging." Magn Reson Med **42**(1): 87-97.

Rinne, T., G. C. Stecker, et al. (2007). "Attention modulates sound processing in human auditory cortex but not the inferior colliculus." Neuroreport **18**(13): 1311-4.

Schulte, A. C., O. Speck, et al. (2001). "Separation and quantification of perfusion and BOLD effects by simultaneous acquisition of functional I(0)- and T2(*)-parameter maps." Magn Reson Med **45**(5): 811-6.

Sigalovsky, I. S. and J. R. Melcher (2006). "Effects of sound level on fMRI activation in human brainstem, thalamic and cortical centers." Hear Res **215**(1-2): 67-76.

Speck, O. and J. Hennig (1998). "Functional imaging by I0- and T2*-parameter mapping using multi-image EPI." Magn Reson Med **40**(2): 243-8.

Thompson, S. K., K. von Kriegstein, et al. (2006). "Representation of interaural time delay in the human auditory midbrain." Nat Neurosci **9**(9): 1096-8.

Wiggins, C. J. and D. G. Norris (1998). Dual-echo EPI: An fMRI method for regions of varying B0 homogeneity. 6th Meeting of the International Society of Magnetic Resonance in Medicine, Sydney, NSW, Australia.

Wilson, E. C., J. R. Melcher, et al. (2007). "Cortical FMRI activation to sequences of tones alternating in frequency: relationship to perceived rate and streaming." J Neurophysiol **97**(3): 2230-8.

Yakolev, P. I. (1970). Whole brain serial histological sections. Neuropathology: Methods and Diagnosis. G. C. Tedeschi. Boston, NY, Little Brown: 371-378.

Zhang, W. T., C. Mainero, et al. (2006). "Strategies for improving the detection of fMRI activation in trigeminal pathways with cardiac gating." Neuroimage **31**(4): 1506-12.

Table 1. *Summary of effects of cardiac gating and T1-correction.*

	T-statistic	*Percent Signal Change*	*Standard Deviation Noise On*	*Standard Deviation Noise Off*
Cochlear Nucleus				
Ungated	2.9 ± 0.89	0.87 ± 0.39	15.2 ± 5.5	15.2 ± 4.7
Gated-Corrected	3.2 ± 1.1	0.74 ± 0.22	12.5 ± 4.3	11.8 ± 3.0
	$p = 0.38$	$p = 0.22$	$p = 0.048$	$p = 0.00024$
Superior Olivary Complex				
Ungated	3.6 ± 0.81	0.71 ± 0.29	11.6 ± 6.8	10.8 ± 6.1
Gated-Corrected	3.2 ± 1.4	0.56 ± 0.28	9.0 ± 3.1	8.6 ± 2.0
	$p = 0.34$	$p = 0.077$	$p = 0.0049$	$p = 0.016$
Inferior Colliculus				
Ungated	3.3 ± 1.3	0.83 ± 0.37	14.9 ± 6.0	15.3 ± 5.2
Gated-Corrected	5.5 ± 1.7	0.91 ± 0.23	8.7 ± 3.4	9.0 ± 2.6
	$p = 0.000080$	$p = 0.092$	$p = 0.000060$	$p = 0.000060$
Medial Geniculate Body				
Ungated	2.6 ± 1.2	0.79 ± 0.36	18.0 ± 7.9	17.2 ± 7.2
Gated-Corrected	3.4 ± 1.2	0.79 ± 0.33	12.2 ± 4.5	12.0 ± 4.6
	$p = 0.10$	$p = 1$	$p = 0.00073$	$p = 0.00024$
Heschl's Gyrus				
Ungated	4.9 ± 1.5	1.1 ± 0.40	11.6 ± 3.8	12.2 ± 3.6
Gated-Corrected	5.3 ± 1.6	1.1 ± 0.30	10.0 ± 3.3	10.5 ± 3.5
	$p = 0.20$	$p = 0.46$	$p = 0.0013$	$p = 0.00025$
Planum Temporale				
Ungated	4.1 ± 1.8	1.2 ± 0.53	15.1 ± 5.4	15.9 ± 5.0
Gated-Corrected	4.1 ± 1.5	1.1 ± 0.56	13.7 ± 4.3	14.2 ± 4.8
	$p = 0.90$	$p = 0.26$	$p = 0.0038$	$p = 0.0019$
Planum Polare				
Ungated	4.4 ± 2.1	1.0 ± 0.61	11.7 ± 4.3	12.6 ± 4.1
Gated-Corrected	4.61 ± 1.9	0.92 ± 0.44	10.4 ± 3.6	10.8 ± 4.1
	$p = 0.65$	$p = 0.29$	$p = 0.0065$	$p = 0.015$

FIGURE CAPTIONS

Figure 1. Acquisition paradigm showing schematic R-wave peaks and the imposed delay (D) between the peak of the R-wave and the start of the image acquisition.

Figure 2. Activation maps from representative subjects chosen because they were around the median in the benefit obtained by cardiac gating. The color code represents level of statistical significance (see text).

Figure 3. Comparisons of (1) T-statistic, (2) percent signal change, (3) signal variability while the stimulus was on and (4) signal variability while the stimulus was off between ungated and gated-corrected acquisition paradigms for all subcortical ROIs. Single and double asterisks indicate significant differences between ungated and gated-corrected conditions for signed-rank and both sign and signed-rank tests, respectively.

Figure 4. Same as figure 3, but for cortical ROIs.

Figure 5. Comparisons of the scatter plots of percent signal change between ungated and gated-corrected conditions for all subcortical ROIs. The gray area in each panel indicates the period during which the stimulus was on.

Figure 6. Same as figure 5, but for cortical ROIs.

Figure 7. Delay between ECG (solid lines) and SpO2 (dotted lines) signals. The left panel shows raw traces of both signals for each of the three subjects. The right panel shows a scatter plot of the delay between the peak of the R-wave and the peak of the SpO2. The mean ± s.d. of the delay is shown in the upper right corner of the right panel.

Figure 8. Simulated minimum percent signal changes (for IC activation detection at the 0.01 level) in each of 8 subjects for both fixed and gated conditions.

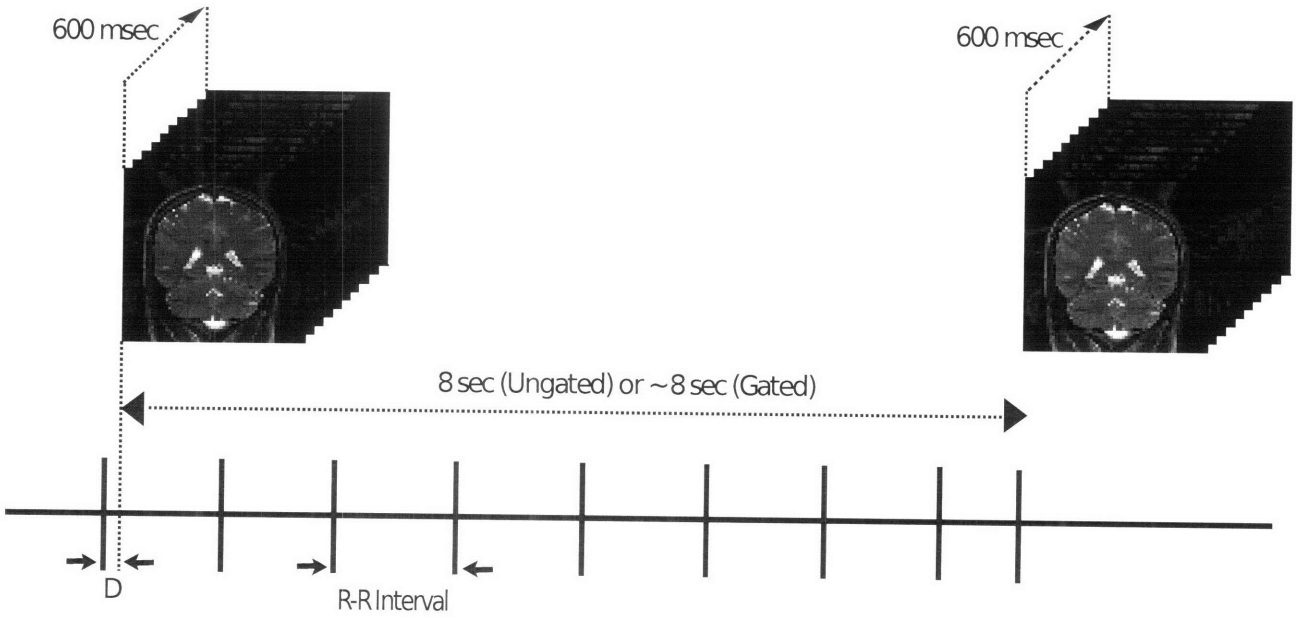
600 msec
600 msec
8 sec (Ungated) or ~8 sec (Gated)
D
R-R Interval

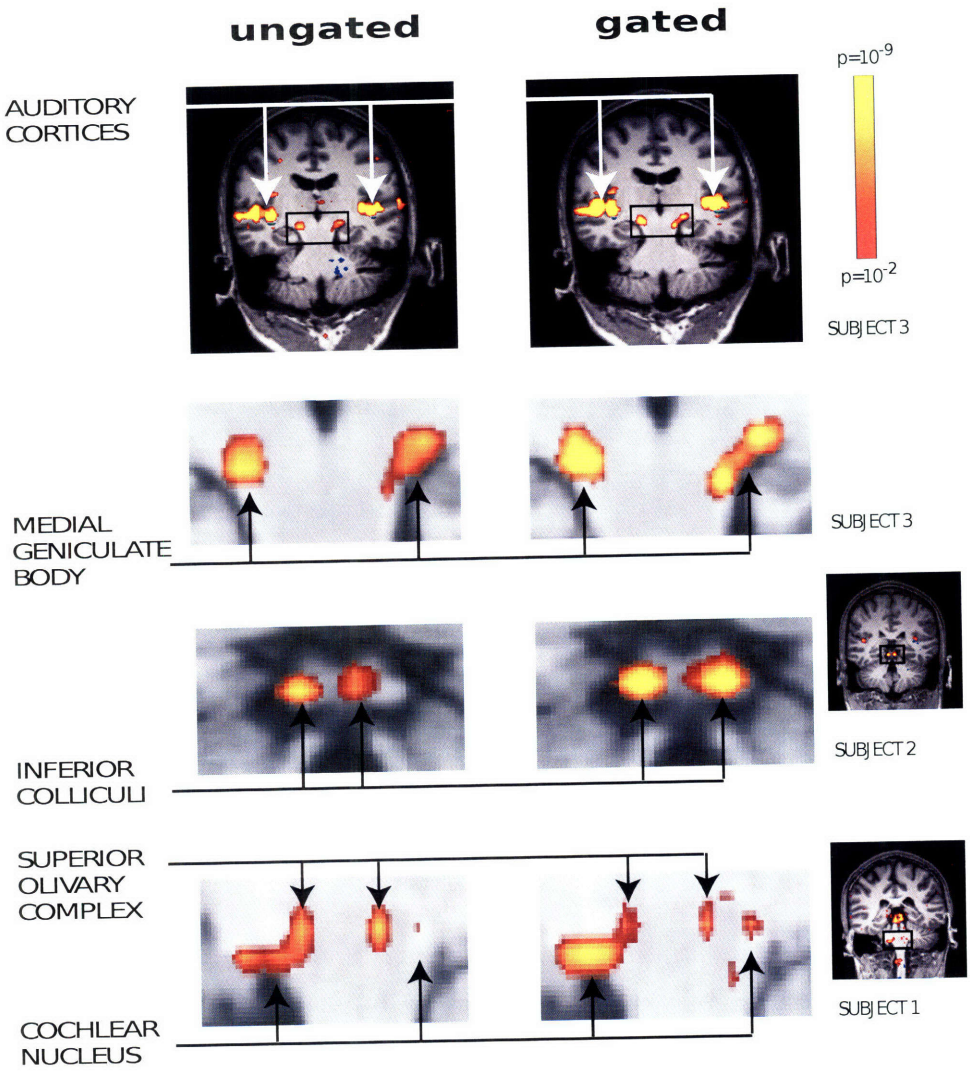
ungated
gated
p=10-9
p=10-2
AUDITORY CORTICES
SUBJECT 3
MEDIAL GENICULATE BODY
SUBJECT 3
INFERIOR COLLICULI
SUBJECT 2
SUPERIOR OLIVARY COMPLEX
COCHLEAR NUCLEUS
SUBJECT 1

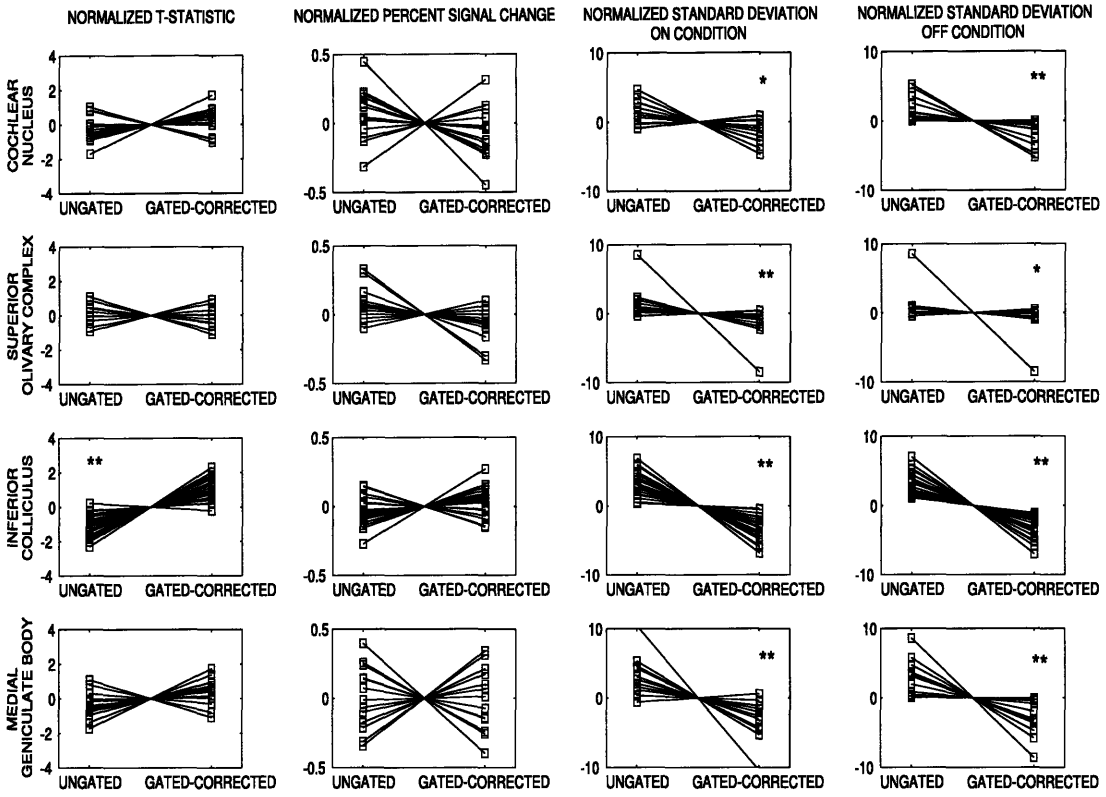
NORMALIZED T-STATISTIC
NORMALIZED PERCENT SIGNAL CHANGE
NORMALIZED STANDARD DEVIATION ON CONDITION
NORMALIZED STANDARD DEVIATION OFF CONDITION
COCHLEAR NUCLEUS
SUPERIOR OLIVARY COMPLEX
INFERIOR COLLICULUS
MEDIAL GENICULATE BODY
UNGATED
GATED-CORRECTED
*
**

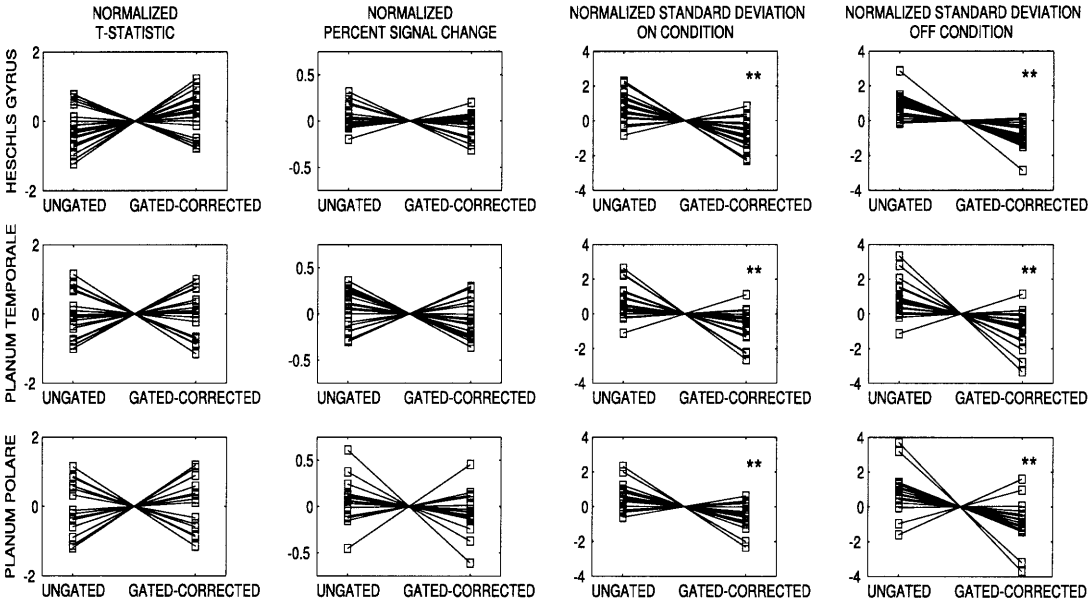
NORMALIZED
T-STATISTIC
NORMALIZED
PERCENT SIGNAL CHANGE
NORMALIZED STANDARD DEVIATION
ON CONDITION
NORMALIZED STANDARD DEVIATION
OFF CONDITION
HESCHLS GYRUS
PLANUM TEMPORALE
PLANUM POLARE
UNGATED
GATED-CORRECTED
**

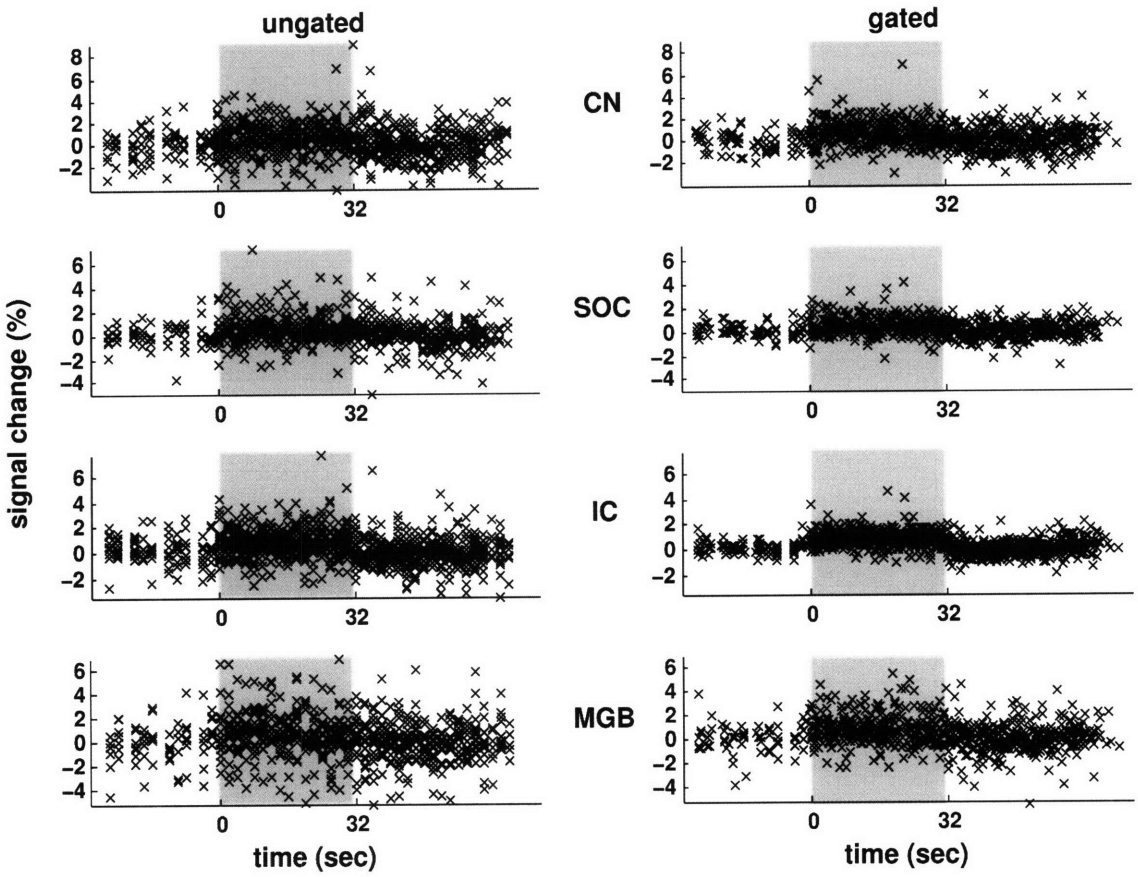
ungated
gated
CN
SOC
IC
MGB
signal change (%)
time (sec)
time (sec)
0
32

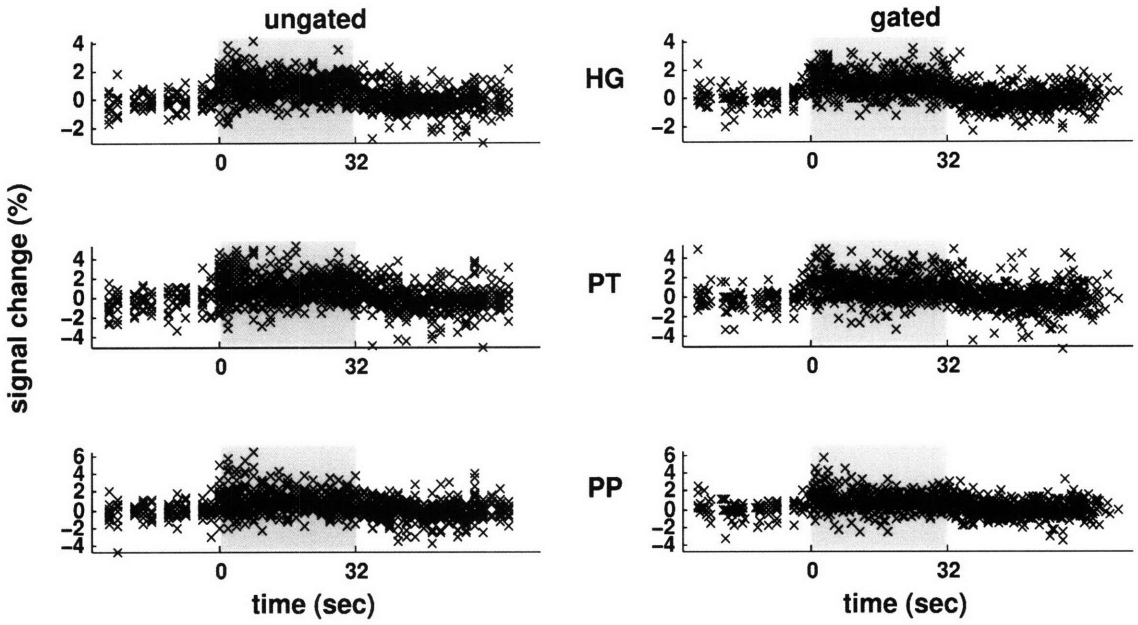
ungated
gated
HG
PT
PP
signal change (%)
time (sec)
time (sec)
0
32

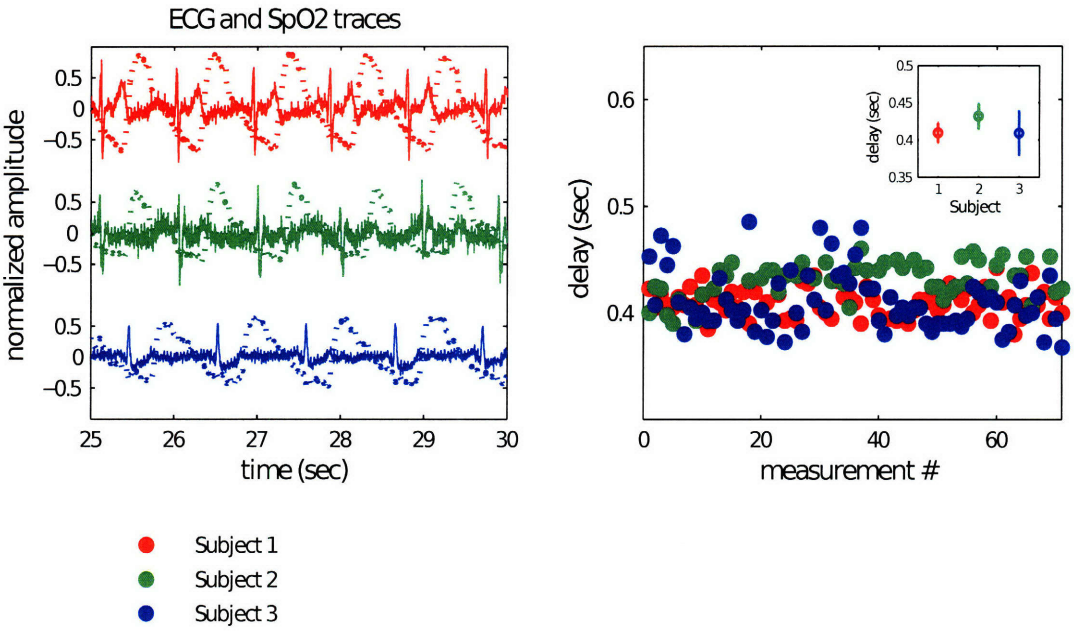
ECG and SpO2 traces
normalized amplitude
0.5
0
−0.5
0.5
0
−0.5
0.5
0
−0.5
25
26
27
28
29
30
time (sec)
delay (sec)
0.6
0.5
0.4
0
20
40
60
measurement #
delay (sec)
0.5
0.45
0.4
0.35
1
2
3
Subject
Subject 1
Subject 2
Subject 3

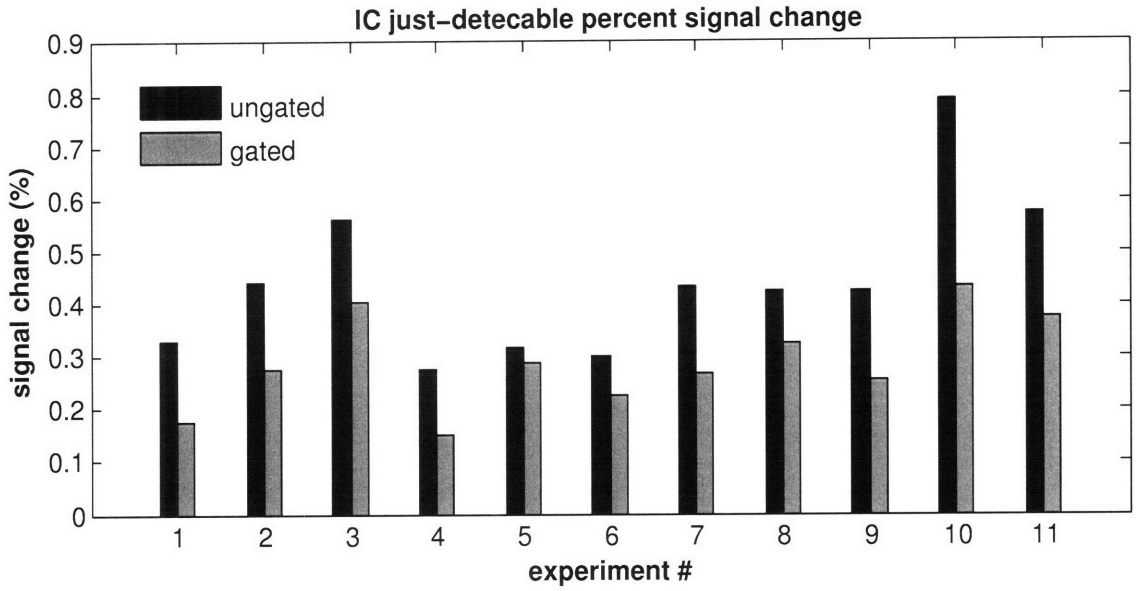
IC just-detecable percent signal change
ungated
gated
signal change (%)
0.9
0.8
0.7
0.6
0.5
0.4
0.3
0.2
0.1
0
1
2
3
4
5
6
7
8
9
10
11
experiment #